



Technical note: Numerical quantification of the mixing states of partially-coated black carbon based on the single-particle soot photometer: Implication for global radiative forcing

Jie Luo¹, Miao Hu¹, Jibing Qiu², Kaitao Li³, Hao He⁴, Yuping Sun⁴, and Xiulin Geng¹

¹College of Communication Engineering, Hangzhou Dianzi University, Hangzhou, Zhejiang, 310018, China.

²Institute of Computing Technology, Chinese Academy of Sciences, Beijing 100190, China

³School of Information, Space Engineering University, Beijing, 101416, China.

⁴China Jiliang University, College of Energy Environment and Safety Engineering, Hangzhou, Zhejiang, China

Correspondence: Jie Luo (luojie@hdu.edu.cn), Miao Hu (miao_hu@hdu.edu.cn)

Abstract.

In this work, we have performed a series of numerical investigations on the mixing states of partially-coated black carbon (BC) based on the single-particle soot photometer (SP2). First, we calculated the scattering signal returned from partially-coated BC based on the SP2 measurement, and then the mixing states were determined using Mie theory, where the difference between the determined and "true" mixing states can represent the uncertainties of the SP2 measurement. We found that the SP2 measurement can provide good estimates for small, heavily coated BCs and shows better performance for fully coated BCs. However, the microphysical properties of BCs have a significant impact on the accuracy of the SP2 measurement; sometimes deviations of about -22% to 28% were observed for the determined particle-to-core size ratio (D_p/D_c). When considering a size distribution, the error in the effective radius is generally within about -17% to 8.8%. We also investigated the effects of Mie-based models using the SP2 determined and volume-mean D_p/D_c on the radiative effects of partially-coated BC. We found that both Mie models based on the volume mean and SP2 determined mixing states overestimate the absorption enhancement (E_{abs}) and direct radiative forcing (DRF) of BC. The Mie model based on the SP2 measurement does not necessarily provide worse estimates of radiative properties, although some errors occur in the determination of the mixing states, since the fraction of the coated core (F) in the particle scale is an important factor affecting E_{abs} and DRF. Sometimes the inaccurate measurements of the mixing states by SP2 would offset the influence of F . Moreover, our results based on the Mie model considering F can significantly improve the estimates for the absorption and DRF of partially-coated BC, although the morphology also has some influence. Therefore, we suggest adding a parameter F to model the radiative effect of BC in climate modeling even when a Mie-based model is used.

1 Introduction

Black carbon (BC), the most important absorbing aerosol in the atmosphere, plays an important role in global warming (Bond et al., 2013; Myhre et al., 2013). BC generally absorbs solar radiation strongly from the UV to the near infrared, so it can lead to a positive radiative forcing in the atmosphere (Bond and Bergstrom, 2006; Cross et al., 2010; Petzold and Schönlinner, 2004).



In addition, other chemical compositions can also be deposited on the BC, which leads to an increase in BC absorption due to the "lens effect" (Adachi et al., 2007; Bond et al., 2013; China et al., 2013; Wang et al., 2021a; Peng et al., 2016; Liu et al., 2017b). There are numerous BC aerosols in the atmosphere, and each BC is coated with different amounts of coating materials (Fierce et al., 2020; Wang et al., 2023). Therefore, BC aerosols generally exhibit complex mixing states, which increases the uncertainties in estimating aerosol absorption and radiative forcing. Understanding the mixing states of coated BC is very important for climate modeling.

The single particle soot photometer (SP2), an instrument for measuring the mass of individual BC particles, has recently been widely used to measure mixing states (Schwarz et al., 2006; R. S. Gao and Worsnop, 2007). The SP2 measures scattering of individual particles reflected from a 1064 nm laser, and the mass of the BC core is estimated from the incandescence signal (Moteki and Kondo, 2008; Wu et al., 2023). Based on an assumed BC mass density, we can calculate the mass-equivalent diameter of the BC cores. In the SP2 algorithm, the total diameter of the particle is usually determined using the complex leading-edge only (LEO) technique, which generally estimates the particle diameter based on the scattering signal (R. S. Gao and Worsnop, 2007; Naseri et al., 2023). However, the SP2 calculation assumes that the particles are spherical and the BC cores are fully coated.

BC aerosols usually have a complex morphology and are often partially-coated (Adachi et al., 2007; China et al., 2013; Wang et al., 2017). Although most researchers have recognized that simplifying the microphysical properties of BC aerosols can lead to inaccurate determination of mixing states, there is still a lack of quantification of the effects of microphysical properties. In some studies, fully enveloped models have been used to determine the effects of BC morphology on the determination of mixing states (Wu et al., 2023; Liu et al., 2023). However, BC is often partially-coated, and the absorption of partially-coated BC is more complex than that of fully coated BC. The absorption of partially-coated BC is determined not only by the ratio of the core volume to the total particle, but also by the ratio of the volume of the coated BC cores to the total volume of the BC cores. In this work, we attempt to quantify the effects of the microphysical properties on the determination of the mixing states of partially-coated BC and present the implications for global radiative forcing calculations. In this work, we mainly focus on answering the following two questions:

- How the microphysical properties of partially-coated BC affect the SP2 retrieval of mixing states?
- How the inaccurate retrieval of mixing states affect the calculations of aerosol absorption and radiative forcing?

2 Methods

2.1 BC morphological model

Freshly emitted BC is commonly composed of numerous near-spherical monomers, and exhibits fluffy structures (China et al., 2013; Chakrabarty et al., 2006; Wentzel et al., 2003b). Previous studies have shown that the fractal law can greatly characterize



the shape of fresh BC (Sorensen, 2001; Heinson et al., 2017; Luo et al., 2021a, b):

$$N_s = k_0 \left(\frac{R_g}{R} \right)^{D_f} \quad (1)$$

where N_s , k_0 and D_f represent monomer number, fractal prefactor and fractal dimension, respectively; R and R_g are the radius of the monomer and the gyration radius, respectively.

D_f and k_0 are two important parameters that reflect the compactness and anisotropy of the particles (Sorensen, 2001; Heinson et al., 2017). For a solid k_0 , the aggregate generally has a more compact structure if it has a larger D_f (Skorupski et al., 2014; Thouy and Jullien, 1994). It is well known that fresh BC has a fluffy structure, and both the numerical simulations and experiments show an approximate D_f of 1.52 – 1.94 in different combustion sources (Sorensen, 2001; Dhaubhadel et al., 2006; China et al., 2013; Chakrabarty et al., 2006; Wentzel et al., 2003b; China et al., 2014). In this work, we used a typical D_f of 1.8 to represent the fresh BC according to Sorensen (2001). As the particle ages, BC may collapse to a more compact structure (Zhang et al., 2008; Lack et al., 2014; Peng et al., 2016; Bhandari et al., 2019). A larger D_f has often been used to represent BC with more compact structure (Liu and Mishchenko, 2005; Kanngießer and Kahnert, 2018; Cheng et al., 2014; Luo et al., 2019, 2023, 2024). Previous studies have shown that aged BC can sometimes have a D_f of about 2.3 – 2.6, assuming a fractal structure for aged BC (Adachi et al., 2010, 2007; Chen et al., 2016). In this work, we have assumed a D_f of 2.6 for compact BC. k_0 is also varied in different regions, but its influence on the optical properties is relatively small, and we only consider a typical value of 1.2 in this work. The BC monomer radius is generally varied in a range of about 8 – 57 nm (Lee et al., 2002; Wentzel et al., 2003a; Mikhailov et al., 2006; Adachi et al., 2007, 2010). However, Kahnert and Kanngießer (2020) has further shown that the typical monomer radius is generally in the range of 10 to 25 nm, and we used an average radius of 20 nm. The monomer number was assumed to be in the range of 5 to 1000, which covers most of the observed BC aerosols.

In the atmosphere, BC can also be mixed internally with other chemical compositions (Adachi et al., 2007; Wang et al., 2021c, b). A special type of internally mixed BC is the partially-coated BC, where only part of the monomers are coated. Not only the BC volume fraction but also the fraction of coated monomers would significantly affect the aerosol absorption. In this work, we mainly consider this type of BC aerosols.

We considered both the effects of BC volume fraction (f_{BC}) of the fraction of coated monomers (F). f_{BC} is represented by the ratio of the volume of BC cores to the total particle:

$$f_{BC} = \frac{V_{BC}}{V_{particle}} \quad (2)$$

where V_{BC} and $V_{particle}$ are the volume of BC core and total particle, respectively.

The particle to core diameter ratio (D_p/D_c) is used to represent the ratio of particle diameter to core diameter:

$$D_p/D_c = \frac{d_{particle}}{d_{BC}} = \left(\frac{1}{f_{BC}} \right)^{1/3} \quad (3)$$

where $d_{particle}$ and d_{BC} are the volume-mean diameter of the total particle and BC core, respectively.

The fraction of coated monomers was represented by the ratio of the volume of coated BC core monomers to total BC core monomers:



$$F = \frac{V_{BC \text{ inside}}}{V_{BC}} \quad (4)$$

where $V_{BC \text{ inside}}$ represents the volume of BC core monomers inside the coating shell, and V_{BC} represent the volume of the total BC core monomers.

We used the tunable algorithm developed by Woźniak (2012), which accurately reproduces the fractal law, to generate the fractal BC aggregates. Then, the coating materials were added similarly to previous studies (Zhang et al., 2018; Luo et al., 2023, 2024). We assumed that the coating structure is spherical. If we know the BC volume fraction (f_{BC}) and F , the spherical shell can be determined. Then, like Zhang et al. (2018), we moved the BC core to find a position where F is satisfied. We moved the BC monomers intersecting with the coating shell out of the coating to use the efficient numerical method, the multiple-sphere T-matrix (MSTM) method (Mackowski and Mishchenko, 2011; Mackowski, 2022), which is only suitable for calculating the optical properties of spheres without overlap. However, previous studies have shown that the motion has no significant effect on the optical properties (Liu et al., 2017a). The typical morphologies are shown in Figure 1. We must clarify that the real coating structure may be more complex than assumed in this work. However, we mainly focus on the effects of the proportion of coated BC monomers and use a typical morphology as an example to illustrate how the mixing states of SP2 are affected by the microphysical properties of BC. The comparison of BC with spherical coating and more complex coating is shown in other studies (Luo et al., 2019).

In this work, we reflect BC with different aging status by the following configurations: (1) fluffy BC aggregates associated with the coating materials, which can be used to represent the fresh BC since they are not internally mixed; (2) compact BC aggregates associated with the coating materials, which is a type of aged BC; (3) Fluffy BC aggregates partially-coated with coating materials, where F and D_p/D_c increase with atmospheric aging; (3) Compact BC aggregates partially-coated with coating materials, where F and D_p/D_c increase with atmospheric aging; (4) Compact BC aggregates fully embedded in the coating shell, representing highly aged BC. SP2 assumed a core-shell BC structure representing only the highly aged BC in determining the indicated mixing. We are trying to better understand the effects microphysical properties at different aging states using the above configurations.

2.2 Calculating of the optical properties of partially-coated BC

The MSTM method, which has an advantage in calculating the optical properties of spheres without overlaps, was used to calculate the optical properties of individual BC aerosols. The MSTM method requires the information of the refractive index and the position of the spheres as input. Bond and Bergstrom (2006) suggested that the refractive index of BC does not vary significantly from ultraviolet (UV) to near infrared (NIR) wavelengths and proposed to use a refractive index of about $1.95 + 0.79i$ at 550 nm. In this work, a fixed BC refractive index $1.95 + 0.79i$ was used for all wavelengths considered in this work. A non-absorbing organic carbon (OC) shell was assumed for the coating materials and the OC refractive index was set to $1.55 + 0i$ (Schnaiter et al., 2005; Bond and Bergstrom, 2006).



2.3 Retrieval of mixing states of partially-coated BC

SP2 determines the particle size based on the scattering signal, which is generally proportional to the scattering cross-sections. Previous studies have shown that SP2 generally detects the scattering signal at scattering angles (Θ) of $45^\circ \pm 32^\circ$ and $135^\circ \pm 32^\circ$ (Moteki and Kondo, 2008; Wu et al., 2023). We used the following equation to represent the scattering signal returned by the coated BC:

$$I_{\text{sca}} \propto C_{\text{sca_det}} = C_{\text{sca}} \sum_{\Theta=0^\circ}^{180^\circ} \omega(\Theta) \sin\Theta P_{11}(\Theta) \quad (5)$$

where I_{sca} represents the detected scattering signal, which is proportional to the detected scattering cross-section at the assumed angles ($C_{\text{sca_det}}$); C_{sca} and P_{11} represent the scattering cross-section and the phase function of the coated BC, respectively. $\omega(\Theta)$ is the weighting function to represent the scattering distribution at different scattering angles, and we used the same $\omega(\Theta)$ as Wu et al. (2023). After calculating $C_{\text{sca_det}}$ of partially-coated BC, the diameter of coated BC is determined based on Mie theory by finding the diameter with the best agreement with $C_{\text{sca_det}}$. In this work, the Mie calculations were performed by PyMieScatt (Sumlin et al., 2018).

Retrieved D_p/D_c (D_p/D_{c_retr}) is determined by:

$$D_p/D_{c_retr} = \frac{d_{\text{particle_retr}}}{d_{\text{BC}}} \quad (6)$$

where $d_{\text{particle_retr}}$ represents the particle diameter determined on the basis of Mie theory.

2.4 Retrieved effective radius of BC with size distributions

There are numerous BC aerosols in the atmosphere, and we have also investigated the determined effective radius of BC with size distributions. We assume a lognormal size distribution for the BC core:

$$n(r_v) = \frac{1}{\sqrt{2\pi}r_v \ln(\sigma_g)} \exp \left[- \left(\frac{\ln(r_v) - \ln(r_g)}{\sqrt{2\ln(\sigma_g)}} \right)^2 \right] \quad (7)$$

where r_g and σ_g are the geometric mean radius and geometric standard deviation, respectively.

The effective radius (R_{eff}) of coated BC is calculated with:

$$R_{\text{eff}} = \frac{\int_{r_{\text{min}}}^{r_{\text{max}}} r_v \pi r_v^2 n(r_v) dr_v}{\int_{r_{\text{min}}}^{r_{\text{max}}} \pi r_v^2 n(r_v) dr_v} \quad (8)$$

2.5 Calculating the absorption enhancement of BC with different mixing states

To evaluate the effects of retrieval uncertainties on radiative forcing, we calculated the bulk absorption enhancement of partially-coated BC and the enhancement calculated with Mie theory based on the retrieved mixing states. Considering the



135 size distribution of the BC core, the absorption enhancement of partially-coated BC ($E_{\text{abs_partially_coated}}$) is calculated as follows:

$$E_{\text{abs_partially_coated}} = \frac{\int_{r_{\min}}^{r_{\max}} C_{\text{abs_partially_coated}}(r_v) n(r_v) dr_v}{\int_{r_{\min}}^{r_{\max}} C_{\text{abs_core}}(r_v) n(r_v) dr_v} \quad (9)$$

where $C_{\text{abs_partially_coated}}$ and $C_{\text{abs_core}}$ represent the absorption cross-section of partially-coated BC and BC core, respectively. The absorption enhancement calculated using Mie theory with the volume-mean diameter can be expressed as:

$$140 \quad E_{\text{abs_core_shell}} = \frac{\int_{r_{\min}}^{r_{\max}} C_{\text{abs_coated_Mie}}(r_v) n(r_v) dr_v}{\int_{r_{\min}}^{r_{\max}} C_{\text{abs_Mie_core}}(r_v) n(r_v) dr_v} \quad (10)$$

where $C_{\text{abs_coated_Mie}}$ and $C_{\text{abs_Mie_core}}$ represent the Mie-based absorption cross-section of coated BC and BC core, respectively.

The absorption enhancement calculated using Mie theory with the retrieved mixing states ($E_{\text{abs_core_shell_retrieved}}$) can be expressed as:

$$145 \quad E_{\text{abs_core_shell_retrieved}} = \frac{\int_{r_{\min}}^{r_{\max}} C_{\text{abs_coated_Mie_retrieved}}(r_v) n(r_v) dr_v}{\int_{r_{\min}}^{r_{\max}} C_{\text{abs_Mie_core}}(r_v) n(r_v) dr_v} \quad (11)$$

where $C_{\text{abs_coated_Mie_retrieved}}$ represents the Mie-based absorption cross-section of coated BC based on the retrieved D_p/D_c .

2.6 Estimating the effects of SP2 retrieval on global radiative effect

In this work, we have investigated the effects of Mie-based models using the mixing states determined in SP2 on global absorption and radiative forcing. First, a global chemistry transport model, the Goddard Earth Observing System with chemistry
150 (GEOS-Chem) model (Bey et al., 2001; Eastham et al., 2018), was used to simulate the BC distribution. The GEOS-Chem simulation was identical to Luo et al. (2024), and a full-chemistry standard simulation was performed for the year 2016. The spatial resolution was set to $4^\circ \times 5^\circ$ and GEOS-Chem was built with 47 vertical layers. Anthropogenic emissions were calculated based on the Community Emissions Data System (CEDS), and emissions from biomass burning were based on the Global Fire Emissions Database (GFED4) inventory (Randerson et al., 2018). The Model of Emissions of Gases and Aerosols
155 from Nature Version 2.1 (MEGAN 2.1) was used to generate the biogenic emissions (Guenther et al., 2012). GEOS-Chem was performed on the basis of MERRA-2 (second Modern-Era Retrospective analysis for Research and Applications) with assimilated meteorology (Molod et al., 2015; Gelaro et al., 2017). After the GEOS-Chem simulation is completed, we can determine the global distribution of BC concentrations. We have taken the temporal average for the BC concentrations over the entire year 2016. Then we can calculate the aerosol optical absorption depth based on the BC mass concentration:

$$160 \quad \text{AAOD}_{\text{BC}} = \text{MAC}_{\text{BC}} \times E_{\text{abs}} \times C_{\text{BC_column}} \quad (12)$$

where $C_{\text{BC_column}}$ is the column mass concentration of BC; MAC_{BC} represents the mass cross-section of the BC core; E_{abs} is the absorption enhancement of coated BC. In principle, MAC_{BC} can be calculated using MSTM or Mie theory. However, an



inconsistency between the modeled and measured MAC_{BC} has been found, and most models underestimate the MAC of BC based on the measured mass density and refractive index (Kahnert, 2010; Luo et al., 2018; Fengshan Liu and Corbin, 2020). In
165 this work, we used a MAC_{BC} of $7.5 \pm 1.2 \text{ m}^2\text{g}^{-1}$ proposed by Bond and Bergstrom (2006).

The direct radiative forcing (DRF) is estimated based on a simple method similar to Kelesidis et al. (2022). Based on the values proposed in Bond et al. (2013), Kelesidis et al. (2022) suggested to use an average absorption forcing efficiency of $170 \pm 43 \text{ Wm}^{-2} / \text{AAOD}$. We estimated the DRF by multiplying the estimated AAOD by $170 \pm 43 \text{ Wm}^{-2} / \text{AAOD}$.

3 Results

170 3.1 The effects of BC microphysical properties on the SP2 retrieved mixing states

Figure 2 shows the retrieved mixing states of BC with different microphysical properties. It can be seen that the determined D_p/D_c does not deviate significantly from the "true" D_p/D_c if the diameter of the BC core size (D_c) is small and the "true" D_p/D_c is large (e.g. $D_p/D_c = 4.6, 2.71$). The deviations are generally within 1%. The possible reason is that the large D_p/D_c and a small BC core cause an overall structure close to the structure of coating materials. The particle structure of small,
175 heavily coated BC is nearly spherical, so the SP2 determination can provide a reasonable estimate. It should be noted that a spherical coating structure was assumed in this work, while actual coated BC may have a more complex structure, which may be a drawback of this study. However, we mainly used a typical morphology as an example to illustrate how the mixing states of SP2 are affected by the microphysical properties of BC, and more complex morphologies may be considered in the future. As the size of the BC core increases, the deviation between "real" and determined D_p/D_c increases, and the relative error can
180 sometimes reach about 28%. In particular, the determined D_p/D_c are randomly distributed if both D_c and D_p/D_c are large. This is because the total particle size is extremely larger when both D_c and D_p/D_c are larger, and at this point the scattering cross-section becomes insensitive to the particle size.

For smaller "true" values D_p/D_c , some obvious deviations are detected, even if D_c is small. The relative error between the "true" and the determined D_p/D_c is generally in a range of about -22% – 8%. BC with larger D_f generally show larger
185 determined D_p/D_c . This is due to the fact that more compact fractal BC aggregates would lead to a larger scattering cross-section and thus to a larger retrieved D_p/D_c . For the fully embedded BC ($F = 1$), the configuration of "Outer" and "Centre" has a significant impact on the retrieved D_p/D_c when D_p/D_c is large (e.g. $D_p/D_c = 4.64$). In general, SP2 retrieval can provide a reasonable estimate for the D_p/D_c of the "centre" configuration if D_c is not large. The relative error between SP2 retrieval and "real" D_p/D_c is generally within 3% for our "centre" configurations when D_c is less than 300 nm. However, the relative
190 error between SP2 retrieval and "real" D_p/D_c can sometimes reach up to 8% for "outer" configurations, which means that the positions of the BC cores can affect the SP2 retrieval accuracy.

Figure 3 – 4 shows the discrepancy between the determined and the "true" effective radius of coated BC with typical size distributions. We found that SP2 overestimates the "true" effective radius for both flaky and compact BC when BC is heavily coated (e.g. $D_p/D_c = 4.64$). The reason for this phenomenon could be that the core-shell-sphere model underestimates
195 the scattering cross-section of heavily coated BC, so a larger size is required to fit the scattering cross-section of partially-



coated BC. Moreover, the overestimation becomes more obvious as r_g and σ_g increase. In general, SP2 retrievals lead to an overestimation of about 0 to 8.8% for heavily coated BC. However, for BC with thin coatings (e.g. $D_p/D_c = 1.49$), the opposite phenomenon was found and the SP2 generally underestimates the "true" effective radius. The scattering cross-section of thin coated BC is generally overestimated by a spherical assumption, resulting in a smaller retrieved size. The phenomenon is similar for BC with a fluffy and compact core. In contrast, SP2 determination significantly underestimates the size of thin-coated BC with a fluffy core. Sometimes the SP2 determination can lead to an underestimation of about 17% for fluffy thin-cored BC (e.g. $D_f = 1.8$, $D_p/D_c = 1.49$), while the underestimation for compact thin-cored BC is within 11% (e.g. $D_f = 2.6$, $D_p/D_c = 1.49$). The reason for this is that the core-shell sphere overestimates the scattering cross-section of thin-coated BC aggregates, leading to an underestimation of the effective BC radius, and that thin-coated, fluffier BC generally has a smaller scattering cross-section, so that the SP2 determination for fluffier BC provides a more significant underestimation.

Figure 5 shows the comparison of E_{abs} of BC with different models, where "partially-coated" represents the E_{abs} partially-coated BC with volume-averaged size; "Mie E_{abs} based on SP2 retrieval" represents the E_{abs} of BC calculated with Mie theory based on SP2 retrieval size; "Mie E_{abs} based on volume-averaged size" represents the E_{abs} of BC calculated with Mie theory based on volume-averaged size. As shown in Figure 5, the core-shell Mie theory significantly overestimates the E_{abs} of partially-coated BC, since the core-shell Mie theory assumes a fully coated structure. In general, Mie-based E_{abs} with SP2 mixed states lead to a relatively lower overestimation than with the "true" mixed states. However, we don't expect a large difference between the Mie-based E_{abs} with SP2 retrieval and the "true" mixing states for fluffy BC (i.e. $D_f = 1.8$), and the difference is generally within 7%. However, sometimes the difference between the Mie-based E_{abs} with SP2 retrieval and the "true" mixing states for compact BC (e.g. $F = 0$, $D_f = 2.6$, $D_p/D_c = 1.49$) can reach about 22%.

3.2 The impact of SP2 retrieval on global radiative effects

Figure 6 compares the global mean AAOD calculated with different configurations, where the meaning of the different configurations is given in Table 1, and "M" stands for Mie theory with the retrieved SP2 size; "M-T" stands for Mie theory with the volume mean size. Previous studies have shown that the overall mean value of AAOD is generally about 0.001 to 0.0029 when a pure BC model is used (Kelesidis et al., 2022; Sand et al., 2021; Kim et al., 2008; Chung and Seinfeld, 2002; Schulz et al., 2006; Textor et al., 2006). However, considering the enhancement of coating materials, the global mean AAOD value could be about 0.0014 to 0.0046. Our simulated global mean AAOD value is generally in the range of 0.0011 to 0.0043, which is generally consistent with values reported in previous studies. We found that the global mean AAOD calculated using Mie theory sometimes reaches about two times. This means that a fully coated Mie theory can lead to a large overestimation of AAOD. We found that the "M" and "M-T" configurations have similar accuracy when the D_p/D_c is large due to an overall spherical morphology. However, significant differences are observed when D_p/D_c is large. The overestimation of AAOD is generally mitigated by using the size obtained with SP2 instead of the mean volume size when F is small (e.g. $F = 0.05$), while sometimes the opposite is observed when F is relatively large (e.g. $F = 0.2$).

Figures 7 – 8 show the estimated DRF comparison with different configurations. citeRN39 showed that coating materials have on average 6.9 times the BC core volume, which corresponds to a typical D_p/D_c of 1.992. Therefore, we have chosen two



Table 1. Case configurations of this work, as shown in Figure 6 and Figure 11.

A	B	C	D	E	F	H	I
F = 0.05	F = 0.05	F = 0.05	F = 0.05	F = 0.2	F = 0.2	F = 0.2	F = 0.2
$f_{BC} = 10\%$	$f_{BC} = 30\%$	$f_{BC} = 10\%$	$f_{BC} = 30\%$	$f_{BC} = 10\%$	$f_{BC} = 20\%$	$f_{BC} = 10\%$	$f_{BC} = 20\%$
$D_f = 1.8$	$D_f = 1.8$	$D_f = 2.6$	$D_f = 2.6$	$D_f = 1.8$	$D_f = 1.8$	$D_f = 2.6$	$D_f = 2.6$

230 typical D_p/D_c of 2.15 and 1.71 for illustration, which can generally reflect the real atmosphere. As can be seen in Figure 8, the DRF of BC is significantly affected by the morphology and F. As expected, for fixed D_p/D_c , the DRF generally increases with increasing F. In addition, Figures 7 – 8 clearly show that both the core-shell model with "True" and the SP2 model significantly overestimate the DRF of partially-coated BC. The DRF difference between the Mie model and the model for partially-coated BC is even comparable to the DRF of partially-coated BC itself. Especially in some regions (e.g. East Asia),

235 the core-shell assumption can overestimate the DRF by more than 10 W/m^2 for partially-coated BC with an F of 0.05 and 0.2. When the BC core is fully coated, the overestimation is relatively attenuated (e.g. $F = 1$, $D_f = 2.6$, Figure 8), and the overestimation is generally within 1 W/m^2 , even in Esat Asia. This is easy to understand since the core-shell model can only represent the fully coated BC. Our simulations show that the DRF difference between the Mie size determined with SP2 and the mean volume size is significantly affected by the D_p/D_c . As shown in Figure 7, the DRF difference between the "CS True"

240 and "SP2" configurations can reach over 2 W/m^2 in some regions (e.g. East Asia) when $D_p/D_c = 1.71$, which is due to the inaccurate determination of SP2. However, the DRF difference between the "CS True" and "SP2" configurations is ignorable when D_p/D_c reaches 2.15, and the difference is generally within 0.1 W/m^2 (see Figure 7). This is because the core-shell structure can generally provide a reasonable estimate for the scattering cross-sections of heavily coated BC, whose overall structure is nearly spherical.

245 3.3 The importance of F in estimating radiative effects

In the calculations above, we have found that the core-shell Mie theory can provide rather inaccurate estimates for the partially-coated BC, using both the retrieved SP2 and the "real" mixing states. However, we found that the effects of core structure are relatively small compared to the proportion of coated core when comparing the cases $D_f = 1.8$, $D_f = 2.6$ and core-shell structure. In application, Mie theory is still a reasonable choice to model aerosol absorption as it is difficult to determine which specific

250 model should be used since BC aerosols have different morphologies. In application, the goal may be to investigate how the Mie model could provide better estimates for the absorption enhancement of partially-coated BC. As shown in Figure 9, we use an uncoated Mie model and a coated Mie model to represent the absorption enhancement of partially-coated BC. The absorption cross-section of the Mie model for individual particles considering the effects of F is expressed as follows:

$$C_{\text{abs_coated}}(r_v, r_p) = C_{\text{abs_coated}}(r_v \times F^{1/3}, r_p) + C_{\text{abs_core}}(r_v \times (1 - F)^{1/3}) \quad (13)$$



255
$$C_{\text{abs_core}}(r_v) = C_{\text{abs_core}}(r_v \times F^{1/3}) + C_{\text{abs_core}}(r_v \times (1 - F)^{1/3}) \quad (14)$$

where $C_{\text{abs_coated}}(r_v, r_p)$ represents the absorption cross-section of coated BC with a core radius of r_v and a shell radius of r_p ; $C_{\text{abs_core}}(r)$ represents the absorption cross-section of coated BC with a core radius of r . It should be noted that the core morphology can also influence the absorption gain. However, we assume that D_p/D_c and F are the two main factors affecting the absorption gain, so our assumption is reasonable for practical application and the effects of core structure will be investigated in other studies.

It is clear from Figure 10 that the performance of the model in estimating the absorption gain of partially-coated BC is significantly improved by adding an F to characterize the absorption at the particle level. Even though the difference between the Mie model and the morphological model is sometimes still about 20%, the performance is significantly better compared to the traditional Mie model. This suggests that our simplified Mie model could be a substitute for the traditional model if we know the F at the particle scale. Especially in field measurements, a fully coated model often overestimates the absorption gain of BC. Many studies have attributed this to the non-uniform mixing states at the particle level. However, more recent studies have also shown that the absorption gain can be overestimated even when the effects of non-uniform mixing conditions are taken into account. The reasons for this probably lie in the partially-coated BC. However, if we use a morphologically realistic model, the calculations are quite computationally intensive, and it is difficult to perform queries to find the F based on the optical measurements and incorporate them into large models (e.g., climate models). Therefore, a simplified model such as our model is a good choice, even if some reasonable error can be introduced.

The global simulations (see Figure 11 – 12) also show that our simplified model can improve the performance of the traditional Mie models when F is taken into account. The global mean AAOD difference between the improved Mie model and the morphologically realistic model is generally within 20%. Moreover, we see that the global AAOD difference calculated using "True" and SP2 computed mixture states is weakened by considering the effects of F and the difference becomes ignorable. A comparison of Figure 12 and Figure 7 also shows that the overestimation of the DRF with the Mie model is significantly weakened by considering the effects of F and the overestimation of the Mie model is generally within $+2 \text{ W/m}^2$, even in highly polluted regions (e.g. East Asia), which is slightly lower than in Figure 7. The DRF difference between the Mie model with "True" and the mixing states determined with SP2 has also decreased to below 0.1 W/m^2 . Therefore, considering F at the particle scale is very important for improving the model performance in estimating the radiation effects, even when using a simplified model. We therefore suggest considering the effects of F in climate modeling, as this is an important factor affecting accuracy.

3.4 Implication for modeling the global direct radiative effect

The mixing states of BC aerosols are one of the most important factors for the uncertainties of climate modeling. In particular, the mixing states would significantly influence the direct radiative effect. In the measurements, the layer thickness parameters (e.g. D_p/D_c) are often used to represent the mixing state. In this work, we conducted a series of numerical investigations on



the effects of the microphysical properties of BC on the mixing states determined by SP2 measurements. We found that the accuracy of SP2 is significantly affected by the microphysical properties of BC, and sometimes a deviation of about -22% to 28% was observed when BC has a partially-coated morphology. This means that the radiation calculations based on SP2 determination would lead to additional uncertainties. However, our results also show that both the core-shell models based on the SP2 measurement and the volume-average model lead to inaccurate estimates of the radiative properties, while the Mie model based on the SP2 measurement does not necessarily provide worse estimates of the radiative properties. The reason for this is that F is the main factor except for D_p/D_c affecting the radiation effects are the F , while the core-shell model assumes a fully-coated structure. Sometimes the inaccurate measurements of the mixing states by SP2 would offset the influence of F . Moreover, our results based on the Mie model considering F can significantly improve the estimates for the absorption and DRF of partially coated BC, even though the morphology also has some influence. Therefore, we suggest adding a parameter F to model the radiative effect of BC in climate modeling even if a Mie-based model is used.

4 Summary and conclusions

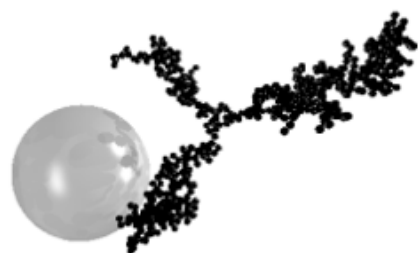
The mixing states of BC play an important role in climate impacts due to the "lensing effect". The SP2 is a commonly used instrument to measure BC concentrations, and it is also commonly used to measure mixture states. However, the mixing states measured with the SP2 are mainly based on the optical retrieval method according to Mie theory. The aerosol is assumed to be spherical, while BC aerosols sometimes have a complex morphology. In this work, a special type of BC aerosol, partially-coated BC, was considered because its absorption is influenced not only by the mixing states but also by F . We first calculate the scattering signal returned from partially-coated BC based on the SP2 measurement, and then the mixing states were retrieved using Mie theory, and the difference between the retrieved and "true" mixing states can be the uncertainties of the SP2 - Represent measurement. Considering different configurations, we investigated the effects of the microphysical properties of BC on the SP2 measurement. We found that the SP2 measurement can provide good estimates for small, heavily coated BCs and shows better performance for fully coated BCs. However, the scattering cross-section is not sensitive to the particle size when the particle size reaches an upper limit, so the SP2 retrieval may produce inaccurate estimates for large heavily coated BC due to the overall extreme large particle size, sometimes the errors can reach about 28%. Furthermore, for thinly coated BC, the SP2 calculation sometimes results in a relative error of about -22% due to the effects of non-spherical morphology. However, when considering a size distribution, the error in effective radius is generally within about -17% to 8.8%.

We also evaluate the performance of the Mie model with "real" and SP2 mixed states. We found that the Mie-based model can lead to inaccurate estimates for the absorption enhancement and DRF of partially-coated BC, and the Mie-based models can generally only represent the fully coated BC. Sometimes the Mie-based global mean AAOD can reach 2 times the value of partially-coated BC, and in some regions (e.g. East Asia) the DRF difference can reach +10 W/m². The difference between the Mie-based AAOD and the DRF is significantly affected by D_p/D_c , and the difference is generally ignorable when D_p/D_c is large for a typical size distribution. However, the DRF difference can reach over 2 W/m² when D_p/D_c is relatively small. The Mie-based model generally provides a better estimate for fully coated BC than for partially-coated BC. We show that the

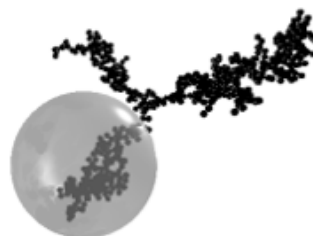


320 performance of the model is significantly improved to reproduce the absorption enhancement and radiative effects of partially-coated BC by including another parameter, F , in the Mie calculations. Therefore, we propose to consider not only the effects of mixing states (D_p/D_c) but also the effects of F for BC aerosols in climate modeling, as recent studies have shown that the Mie-based E_{abs} sometimes still overestimates the measured values, even if the non-uniform mixing conditions are taken into account.

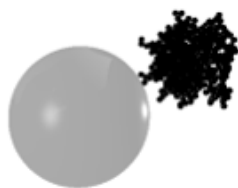
325 *Acknowledgements.* This work was financially supported by the National Natural Science Foundation of China (Grant No. 42305148, 42175146) and the primary Research and Development Plan of Zhejiang Province (Grant No. 2023C03014, 2024C03252).



(a) $D_f = 1.8, F = 0$



(b) $D_f = 1.8, F = 0.3$



(c) $D_f = 2.6, F = 0$



(b) $D_f = 2.6, F = 0.3$

Figure 1. Typical morphologies of coated BC considered in this work.

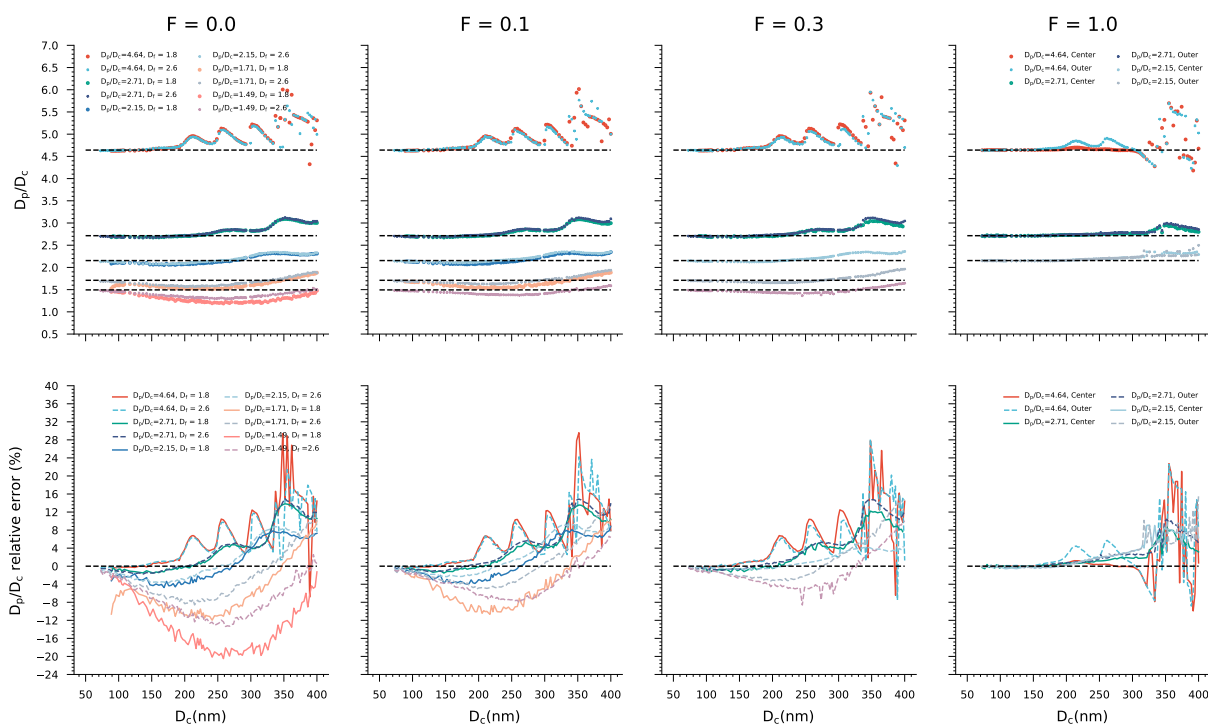


Figure 2. The retrieved D_p/D_c of BC with different microphysical properties. SP2 retrieval can generally provide relatively good estimates when the BC kernel size (D_c) is small and the "true" D_p/D_c is large. In other cases, however, the accuracy of the SP2 determination is significantly influenced by the microphysical properties of the BC.

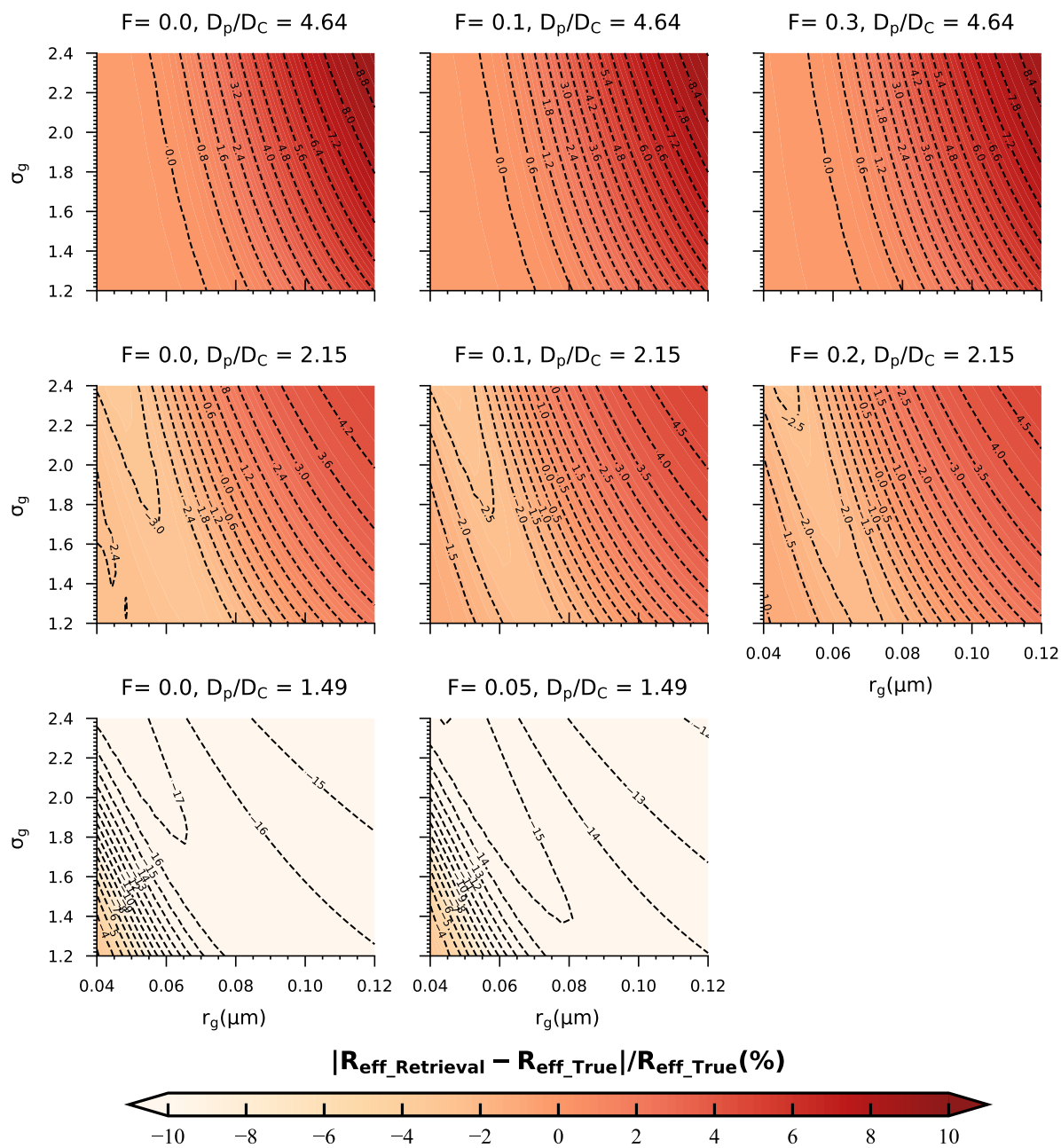


Figure 3. The difference between SP2 retrieved and "True" effective radius (R_{eff}), where $D_f = 1.8$.

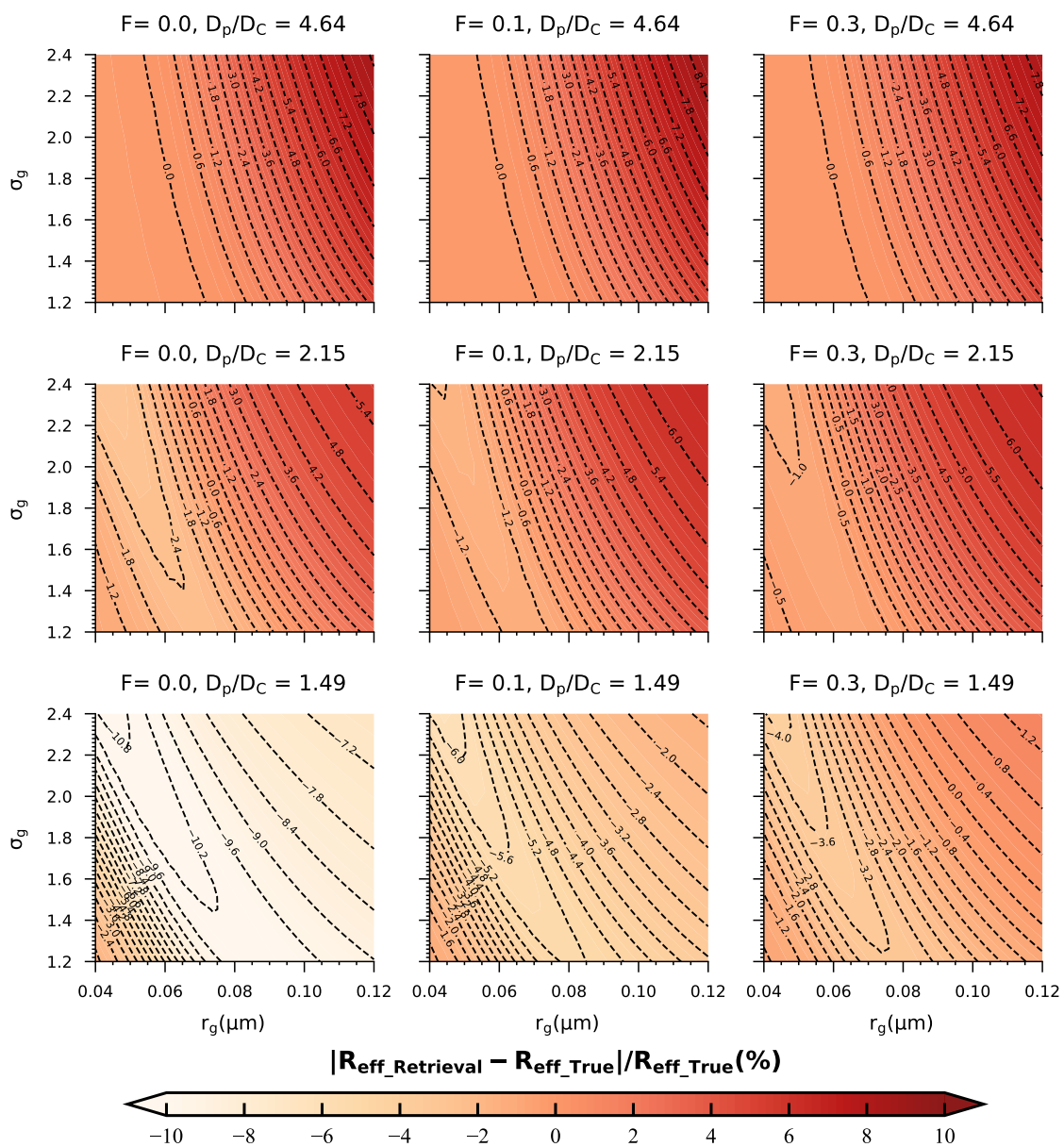


Figure 4. Similar to Figure 3, but for $D_f = 2.6$.

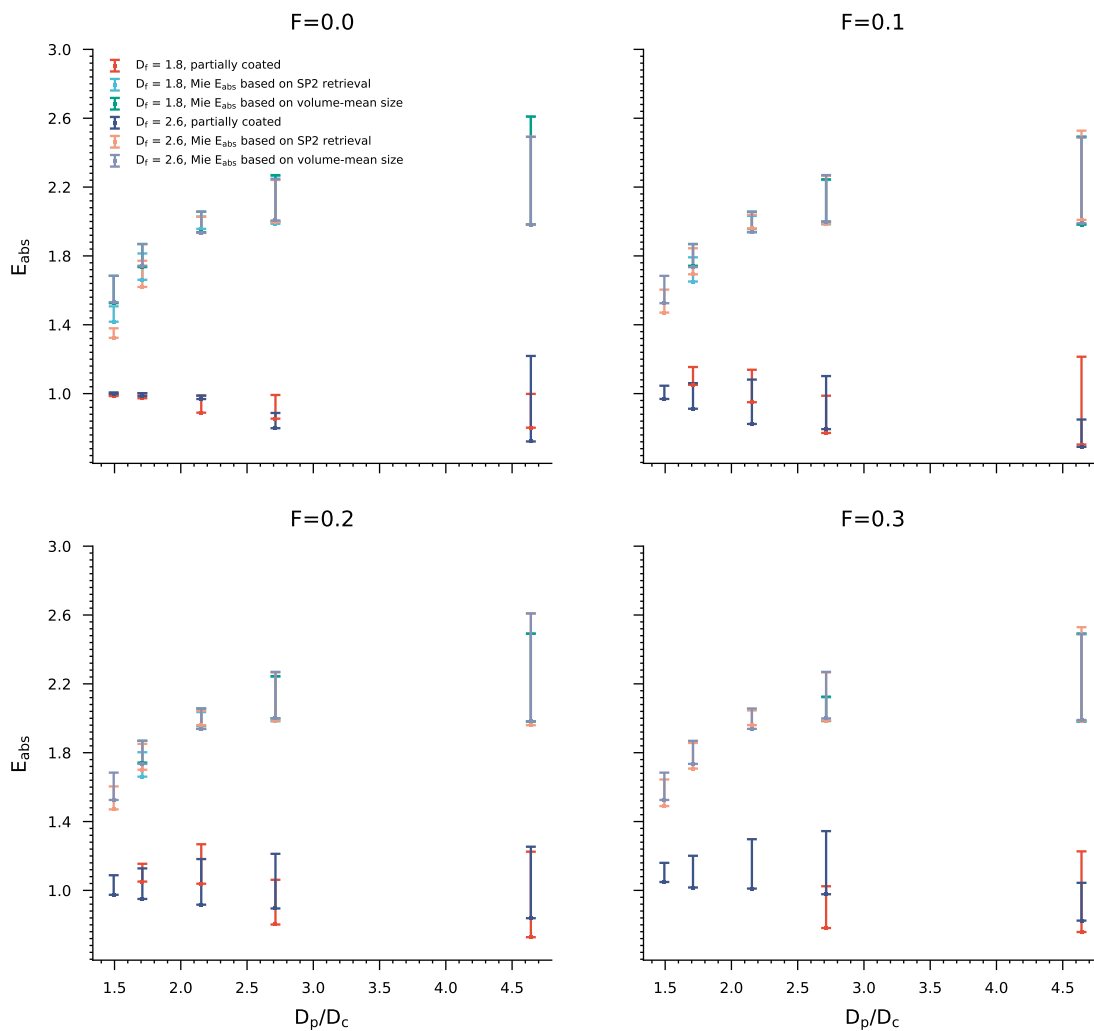


Figure 5. The comparison of E_{abs} modeled with morphologically realistic models, Mie models based on the SP2 retrieved and "true" mixing states. Mie-based models significantly overestimate the E_{abs} of partially-coated BC due to the assumption of fully coated BC.

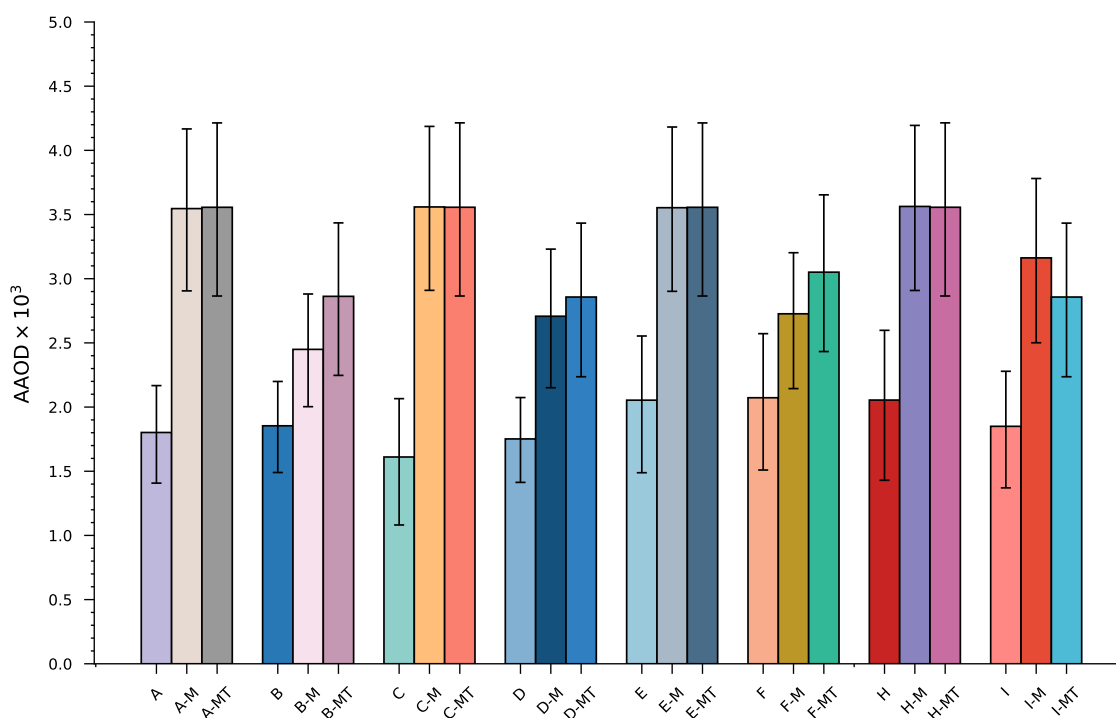


Figure 6. Comparing the global mean of AAOD modeled with morphologically realistic models, Mie models based on the SP2, and "true" mixing states. Mie-based models significantly overestimate the AAOD of partially-coated BC due to the assumption of fully coated BC, and the difference between Mie-based models based on SP2 retrieved and "true" D_p/D_c .

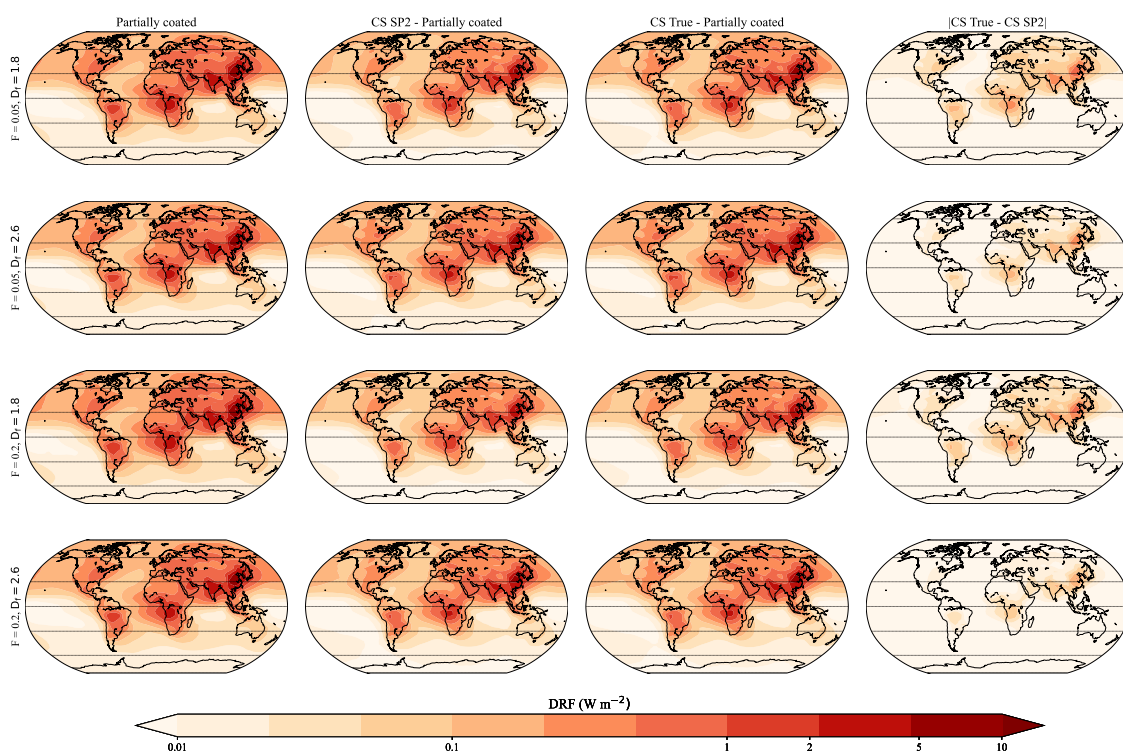


Figure 7. Comparisons of the global mean DRF modeled with morphologically realistic models, Mie models based on the SP2, and "true" mixing states, where f_{BC} is 20%. The DRF overestimation of Mie models are even comparable to that of partially-coated BC itself. The DRF was calculated by multiplying the AAOD by $170 \pm 43 \text{ W m}^{-2} / \text{AAOD}$ and the contour shows the median values.

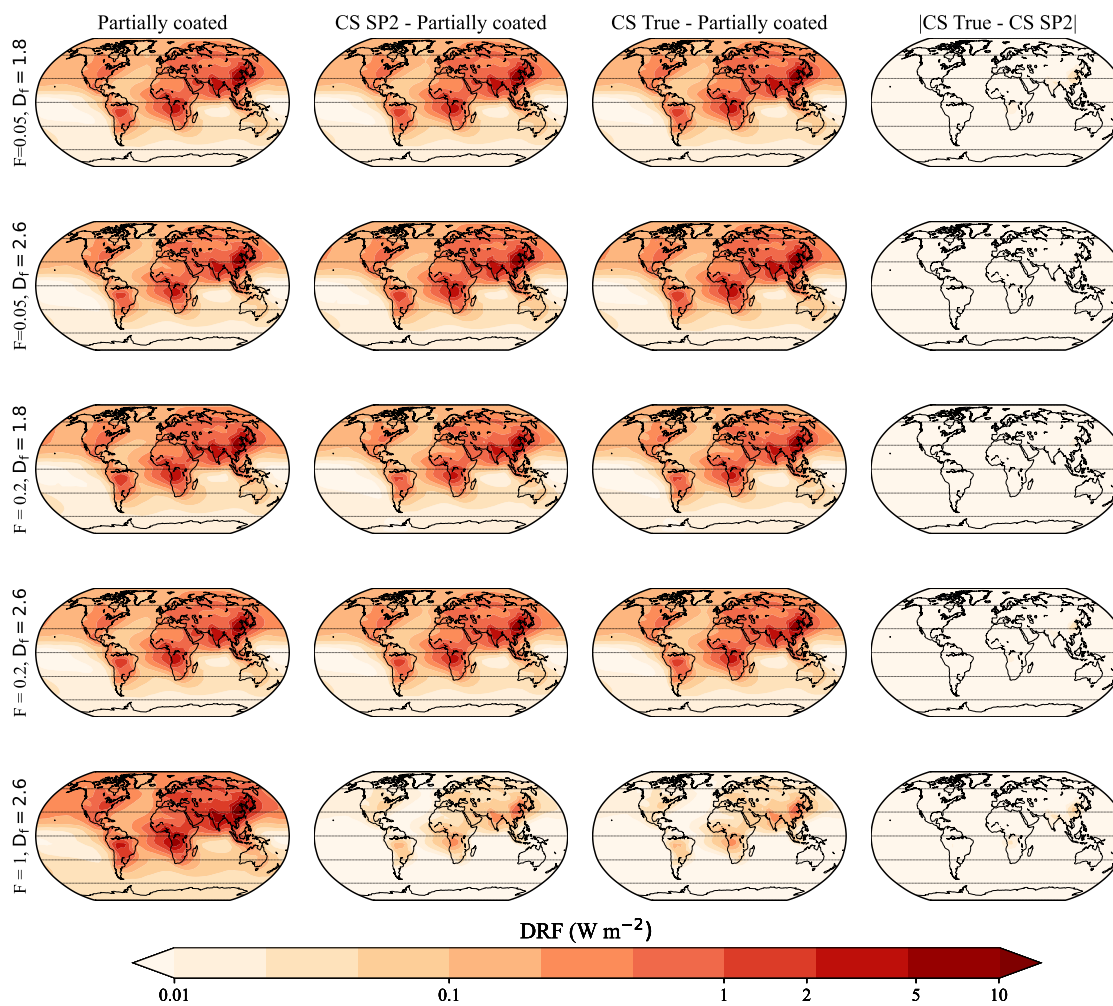


Figure 8. Similar to Figure 7, but for $f_{BC} = 10\%$. It can be seen that the DRF difference between Mie models based on SP2 and "True" D_p/D_c is smaller than in cases where $f_{BC} = 20\%$.

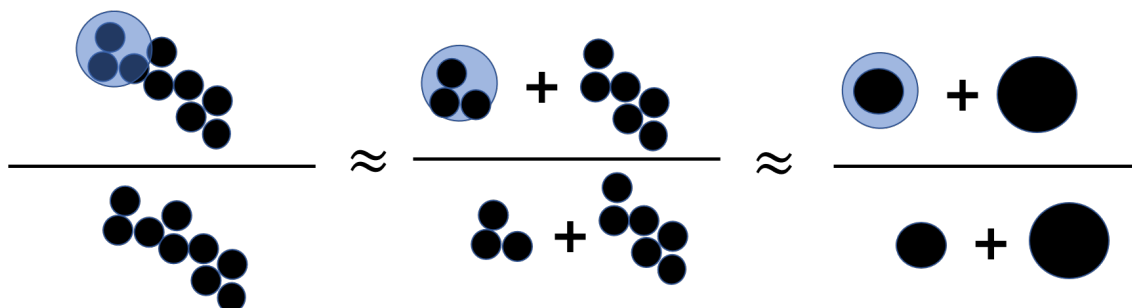


Figure 9. Improved Mie model by considering an additional parameter that characterizes the proportion of the coated BC core (F).

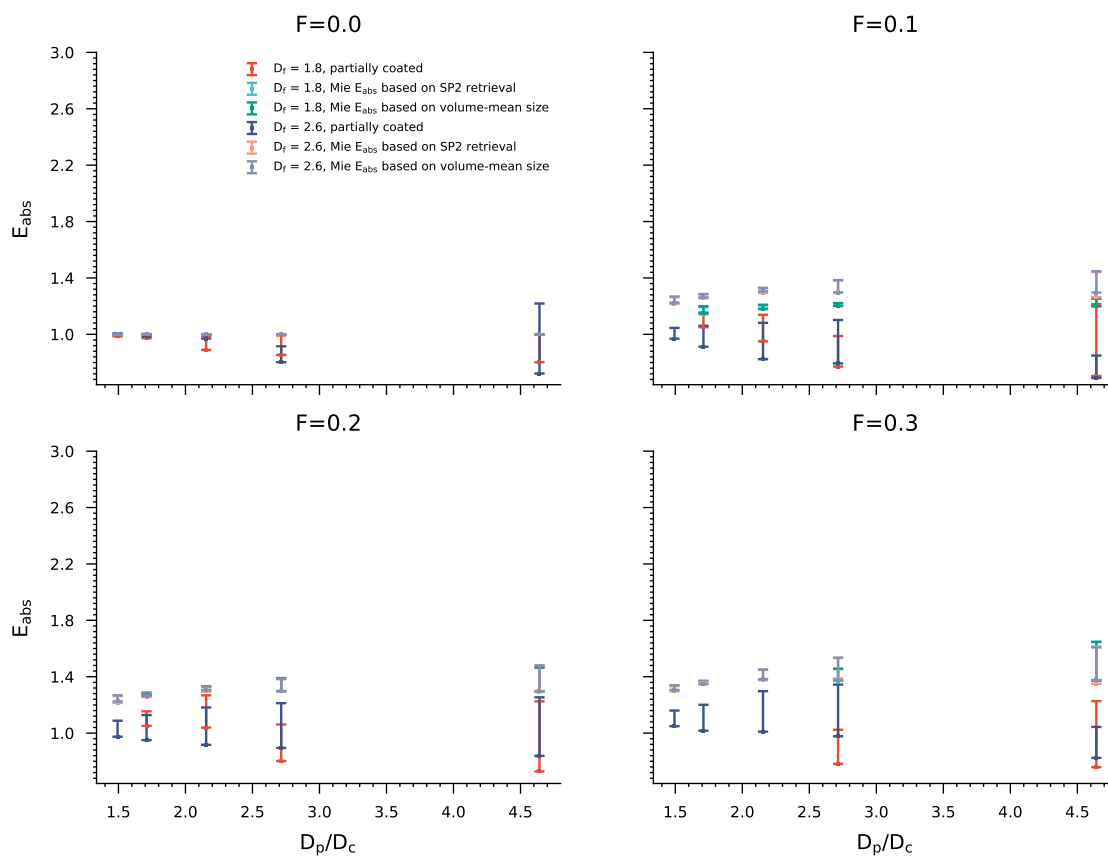


Figure 10. Similar to Figure 5, but taking into account the effects of F in the Mie models. The results show that the accuracy of the Mie-based E_{abs} models is significantly improved when we consider external parameters to describe the effects of F .

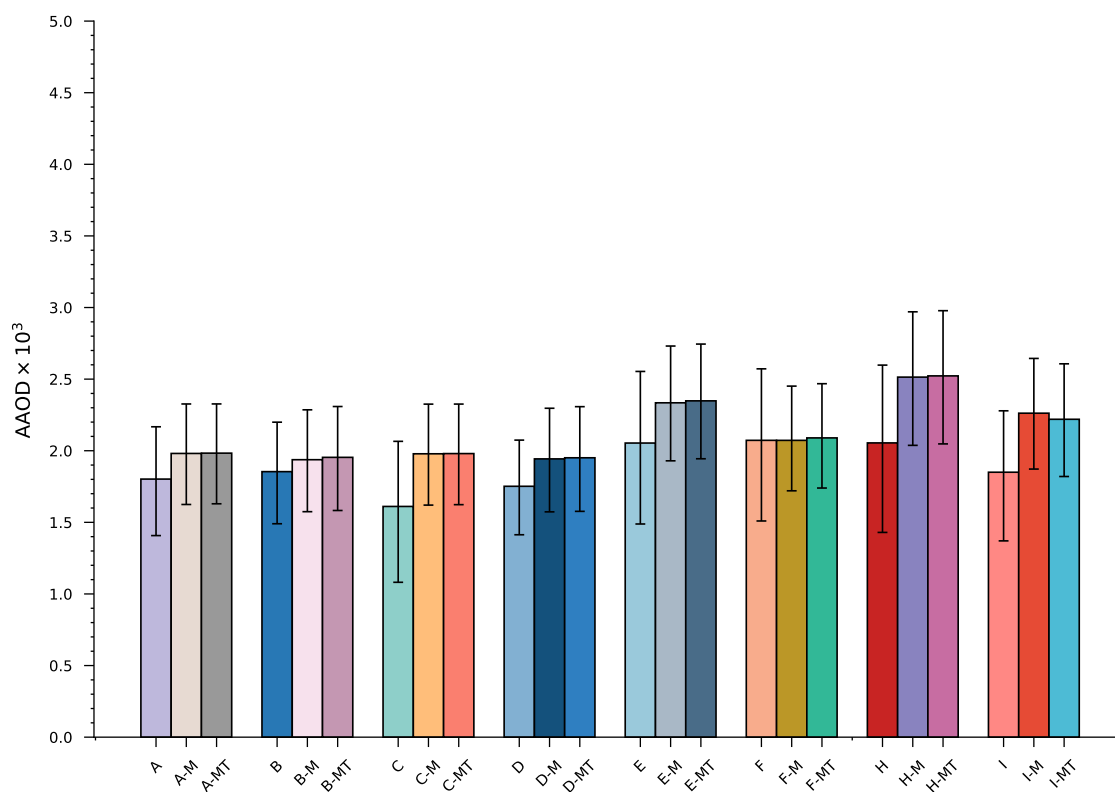


Figure 11. Similar to Figure 6, but taking into account the effects of F in the Mie models.

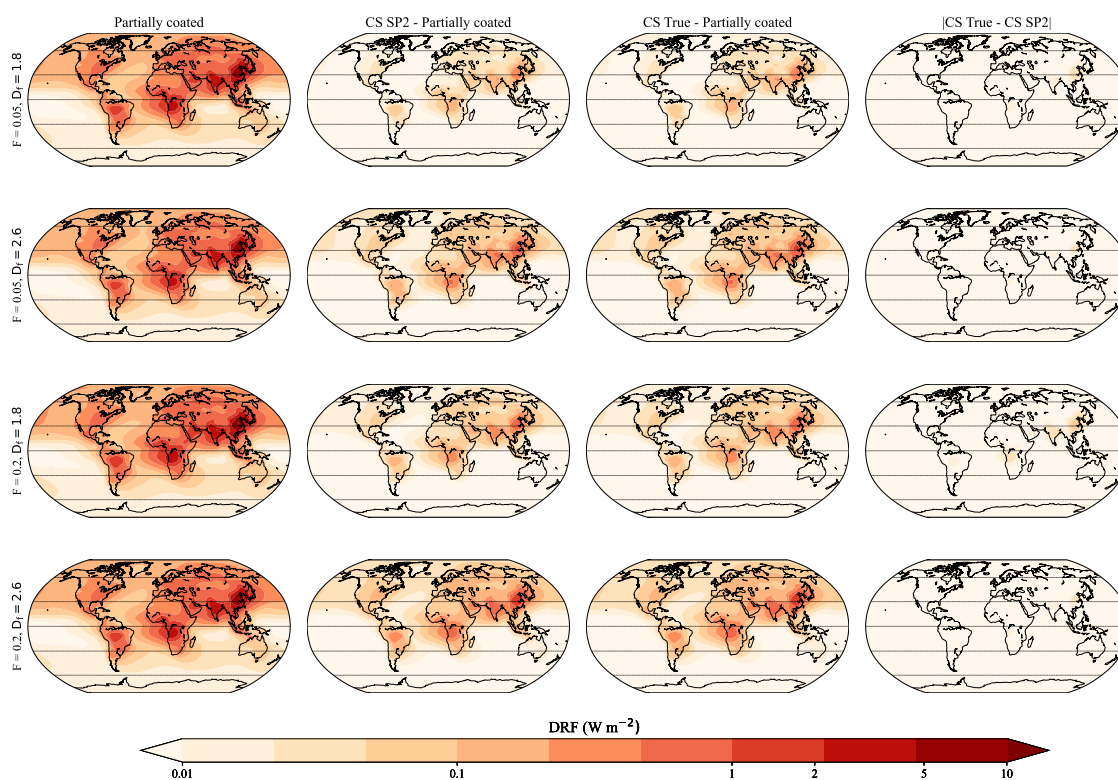


Figure 12. Similar to Figure 8, but taking into account the effects of F in the Mie models.



References

- Adachi, K., Chung, S. H., Friedrich, H., and Buseck, P. R.: Fractal parameters of individual soot particles determined using electron tomography: Implications for optical properties, *Journal of Geophysical Research: Atmospheres*, 112, <https://doi.org/https://doi.org/10.1029/2006JD008296>, 2007.
- Adachi, K., Chung, S. H., and Buseck, P. R.: Shapes of soot aerosol particles and implications for their effects on climate, *Journal of Geophysical Research: Atmospheres*, 115, <https://doi.org/https://doi.org/10.1029/2009JD012868>, 2010.
- Bey, I., Jacob, D. J., Yantosca, R. M., Logan, J. A., Field, B. D., Fiore, A. M., Li, Q., Liu, H. Y., Mickley, L. J., and Schultz, M. G.: Global modeling of tropospheric chemistry with assimilated meteorology: Model description and evaluation, *Journal of Geophysical Research: Atmospheres*, 106, 23 073–23 095, <https://doi.org/https://doi.org/10.1029/2001JD000807>, 2001.
- Bhandari, J., China, S., Chandrakar, K. K., Kinney, G., Cantrell, W., Shaw, R. A., Mazzoleni, L. R., Giroto, G., Sharma, N., Gorkowski, K., et al.: Extensive soot compaction by cloud processing from laboratory and field observations, *Scientific reports*, 9, 11 824, 2019.
- Bond, T. C. and Bergstrom, R. W.: Light Absorption by Carbonaceous Particles: An Investigative Review, *Aerosol Science and Technology*, 40, 27–67, <https://doi.org/10.1080/02786820500421521>, 2006.
- Bond, T. C., Doherty, S. J., Fahey, D. W., Forster, P. M., Berntsen, T., DeAngelo, B. J., Flanner, M. G., Ghan, S., Kärcher, B., Koch, D., Kinne, S., Kondo, Y., Quinn, P. K., Sarofim, M. C., Schultz, M. G., Schulz, M., Venkataraman, C., Zhang, H., Zhang, S., Bellouin, N., Guttikunda, S. K., Hopke, P. K., Jacobson, M. Z., Kaiser, J. W., Klimont, Z., Lohmann, U., Schwarz, J. P., Shindell, D., Storelvmo, T., Warren, S. G., and Zender, C. S.: Bounding the role of black carbon in the climate system: A scientific assessment, *Journal of Geophysical Research: Atmospheres*, 118, 5380–5552, <https://doi.org/https://doi.org/10.1002/jgrd.50171>, 2013.
- Chakrabarty, R. K., Moosmüller, H., Garro, M. A., Arnott, W. P., Walker, J., Susott, R. A., Babbitt, R. E., Wold, C. E., Lincoln, E. N., and Hao, W. M.: Emissions from the laboratory combustion of wildland fuels: Particle morphology and size, *Journal of Geophysical Research: Atmospheres*, 111, <https://doi.org/https://doi.org/10.1029/2005JD006659>, 2006.
- Chen, C., Fan, X., Shaltout, T., Qiu, C., Ma, Y., Goldman, A., and Khalizov, A. F.: An unexpected restructuring of combustion soot aggregates by subnanometer coatings of polycyclic aromatic hydrocarbons, *Geophysical Research Letters*, 43, 11,080–11,088, <https://doi.org/https://doi.org/10.1002/2016GL070877>, 2016.
- Cheng, T., Wu, Y., and Chen, H.: Effects of morphology on the radiative properties of internally mixed light absorbing carbon aerosols with different aging status, *Opt. Express*, 22, 15 904–15 917, <https://doi.org/10.1364/OE.22.015904>, 2014.
- China, S., Mazzoleni, C., Gorkowski, K., Aiken, A. C., and Dubey, M. K.: Morphology and mixing state of individual freshly emitted wildfire carbonaceous particles, *Nature communications*, 4, 1–7, 2013.
- China, S., Salvadori, N., and Mazzoleni, C.: Effect of traffic and driving characteristics on morphology of atmospheric soot particles at freeway on-ramps, *Environmental science & technology*, 48, 3128–3135, 2014.
- Chung, S. H. and Seinfeld, J. H.: Global distribution and climate forcing of carbonaceous aerosols, *Journal of Geophysical Research: Atmospheres*, 107, AAC 14–1–AAC 14–33, <https://doi.org/https://doi.org/10.1029/2001JD001397>, 2002.
- Cross, E. S., Onasch, T. B., Ahern, A., Wrobel, W., Slowik, J. G., Olfert, J., Lack, D. A., Massoli, P., Cappa, C. D., Schwarz, J. P., Spackman, J. R., Fahey, D. W., Sedlacek, A., Trimborn, A., Jayne, J. T., Freedman, A., Williams, L. R., Ng, N. L., Mazzoleni, C., Dubey, M., Brem, B., Kok, G., Subramanian, R., Freitag, S., Clarke, A., Thornhill, D., Marr, L. C., Kolb, C. E., Worsnop, D. R., and Davidovits, P.: Soot Particle Studies—Instrument Inter-Comparison—Project Overview, *Aerosol Science and Technology*, 44, 592–611, <https://doi.org/10.1080/02786826.2010.482113>, 2010.



- 365 Dhaubhadel, R., Pierce, F., Chakrabarti, A., and Sorensen, C.: Hybrid superaggregate morphology as a result of aggregation in a cluster-dense aerosol, *Physical Review E*, 73, 011 404, 2006.
- Eastham, S. D., Long, M. S., Keller, C. A., Lundgren, E., Yantosca, R. M., Zhuang, J., Li, C., Lee, C. J., Yannetti, M., Auer, B. M., Clune, T. L., Kouatchou, J., Putman, W. M., Thompson, M. A., Trayanov, A. L., Molod, A. M., Martin, R. V., and Jacob, D. J.: GEOS-Chem High Performance (GCHP v11-02c): a next-generation implementation of the GEOS-Chem chemical transport model for massively parallel applications, *Geoscientific Model Development*, 11, 2941–2953, <https://doi.org/10.5194/gmd-11-2941-2018>, 2018.
- 370 Fengshan Liu, Jérôme Yon, A. F. P. L. G. J. S. and Corbin, J. C.: Review of recent literature on the light absorption properties of black carbon: Refractive index, mass absorption cross section, and absorption function, *Aerosol Science and Technology*, 54, 33–51, <https://doi.org/10.1080/02786826.2019.1676878>, 2020.
- Fierce, L., Onasch, T. B., Cappa, C. D., Mazzoleni, C., China, S., Bhandari, J., Davidovits, P., Fischer, D. A., Helgestad, T., Lambe, A. T., Sedlacek, A. J., Smith, G. D., and Wolff, L.: Radiative absorption enhancements by black carbon controlled by particle-to-particle heterogeneity in composition, *Proceedings of the National Academy of Sciences*, 117, 5196–5203, <https://doi.org/10.1073/pnas.1919723117>, 2020.
- 375 Gelaro, R., McCarty, W., Suárez, M. J., Todling, R., Molod, A., Takacs, L., Randles, C. A., Darmenov, A., Bosilovich, M. G., Reichle, R., Wargan, K., Coy, L., Cullather, R., Draper, C., Akella, S., Buchard, V., Conaty, A., da Silva, A. M., Gu, W., Kim, G.-K., Koster, R., Lucchesi, R., Merkova, D., Nielsen, J. E., Partyka, G., Pawson, S., Putman, W., Rienecker, M., Schubert, S. D., Sienkiewicz, M., and Zhao, B.: The Modern-Era Retrospective Analysis for Research and Applications, Version 2 (MERRA-2), *Journal of Climate*, 30, 5419 – 5454, <https://doi.org/https://doi.org/10.1175/JCLI-D-16-0758.1>, 2017.
- Guenther, A. B., Jiang, X., Heald, C. L., Sakulyanontvittaya, T., Duhl, T., Emmons, L. K., and Wang, X.: The Model of Emissions of Gases and Aerosols from Nature version 2.1 (MEGAN2.1): an extended and updated framework for modeling biogenic emissions, *Geoscientific Model Development*, 5, 1471–1492, <https://doi.org/10.5194/gmd-5-1471-2012>, 2012.
- 385 Heinson, W. R., Liu, P., and Chakrabarty, R. K.: Fractal scaling of coated soot aggregates, *Aerosol Science and Technology*, 51, 12–19, 2017.
- Kahnert, M.: On the Discrepancy between Modeled and Measured Mass Absorption Cross Sections of Light Absorbing Carbon Aerosols, *Aerosol Science and Technology*, 44, 453–460, <https://doi.org/10.1080/02786821003733834>, 2010.
- Kahnert, M. and Kanngießer, F.: Modelling optical properties of atmospheric black carbon aerosols, *Journal of Quantitative Spectroscopy and Radiative Transfer*, 244, 106 849, <https://doi.org/https://doi.org/10.1016/j.jqsrt.2020.106849>, 2020.
- 390 Kanngießer, F. and Kahnert, M.: Calculation of optical properties of light-absorbing carbon with weakly absorbing coating: A model with tunable transition from film-coating to spherical-shell coating, *Journal of Quantitative Spectroscopy and Radiative Transfer*, 216, 17–36, <https://doi.org/https://doi.org/10.1016/j.jqsrt.2018.05.014>, 2018.
- Kelesidis, G. A., Neubauer, D., Fan, L.-S., Lohmann, U., and Pratsinis, S. E.: Enhanced Light Absorption and Radiative Forcing by Black Carbon Agglomerates, *Environmental Science & Technology*, 56, 8610–8618, <https://doi.org/10.1021/acs.est.2c00428>, 2022.
- 395 Kim, D., Wang, C., Ekman, A. M. L., Barth, M. C., and Rasch, P. J.: Distribution and direct radiative forcing of carbonaceous and sulfate aerosols in an interactive size-resolving aerosol–climate model, *Journal of Geophysical Research: Atmospheres*, 113, <https://doi.org/https://doi.org/10.1029/2007JD009756>, 2008.
- Lack, D. A., Moosmüller, H., McMeeking, G. R., Chakrabarty, R. K., and Baumgardner, D.: Characterizing elemental, equivalent black, and refractory black carbon aerosol particles: a review of techniques, their limitations and uncertainties, *Analytical and bioanalytical chemistry*, 406, 99–122, 2014.
- 400



- Lee, K. O., Cole, R., Sekar, R., Choi, M. Y., Kang, J. S., Bae, C. S., and Shin, H. D.: Morphological investigation of the microstructure, dimensions, and fractal geometry of diesel particulates, *Proceedings of the Combustion Institute*, 29, 647–653, [https://doi.org/https://doi.org/10.1016/S1540-7489\(02\)80083-9](https://doi.org/https://doi.org/10.1016/S1540-7489(02)80083-9), proceedings of the Combustion Institute, 2002.
- Liu, C., Li, J., Yin, Y., Zhu, B., and Feng, Q.: Optical properties of black carbon aggregates with non-absorptive coating, *Journal of Quantitative Spectroscopy and Radiative Transfer*, 187, 443–452, <https://doi.org/https://doi.org/10.1016/j.jqsrt.2016.10.023>, 2017a.
- Liu, D., Whitehead, J., Alfarrá, M. R., Reyes-Villegas, E., Spracklen, D., Reddington, C., Kong, S., Williams, P., Ting, Y.-C., Haslett, S., Taylor, J., Flynn, M., Morgan, W., McFiggans, G., Coe, H., and Allan, J.: Black-carbon absorption enhancement in the atmosphere determined by particle mixing state, *Nature Geoscience*, 10, 184–188, <https://doi.org/10.1038/ngeo2901>, 2017b.
- Liu, J., Wang, G., Zhu, C., Zhou, D., and Wang, L.: Numerical investigation on retrieval errors of mixing states of fractal black carbon aerosols using single-particle soot photometer based on Mie scattering and the effects on radiative forcing estimation, *Atmospheric Measurement Techniques*, 16, 4961–4974, <https://doi.org/10.5194/amt-16-4961-2023>, 2023.
- Liu, L. and Mishchenko, M. I.: Effects of aggregation on scattering and radiative properties of soot aerosols, *Journal of Geophysical Research: Atmospheres*, 110, <https://doi.org/https://doi.org/10.1029/2004JD005649>, 2005.
- Luo, J., Zhang, Y., Wang, F., and Zhang, Q.: Effects of brown coatings on the absorption enhancement of black carbon: a numerical investigation, *Atmospheric Chemistry and Physics*, 18, 16 897–16 914, <https://doi.org/10.5194/acp-18-16897-2018>, 2018.
- Luo, J., Zhang, Q., Luo, J., Liu, J., Huo, Y., and Zhang, Y.: Optical Modeling of Black Carbon With Different Coating Materials: The Effect of Coating Configurations, *Journal of Geophysical Research: Atmospheres*, 124, 13 230–13 253, <https://doi.org/https://doi.org/10.1029/2019JD031701>, 2019.
- Luo, J., Zhang, Q., Zhang, C., Zhang, Y., and Chakrabarty, R. K.: The fractal characteristics of atmospheric coated soot: Implication for morphological analysis, *Journal of Aerosol Science*, 157, 105 804, <https://doi.org/https://doi.org/10.1016/j.jaerosci.2021.105804>, 2021a.
- Luo, J., Zhang, Q., Zhang, Y., and Li, Z.: Radiative Properties of Non-spherical Black Carbon Aerosols, pp. 69–124, Springer International Publishing, Cham, https://doi.org/10.1007/978-3-030-87683-8_3, 2021b.
- Luo, J., Li, Z., Qiu, J., Zhang, Y., Fan, C., Li, L., Wu, H., Zhou, P., Li, K., and Zhang, Q.: The Simulated Source Apportionment of Light Absorbing Aerosols: Effects of Microphysical Properties of Partially-Coated Black Carbon, *Journal of Geophysical Research: Atmospheres*, 128, e2022JD037 291, <https://doi.org/https://doi.org/10.1029/2022JD037291>, e2022JD037291 2022JD037291, 2023.
- Luo, J., Li, D., Wang, Y., Sun, D., Hou, W., Ren, J., Wu, H., Zhou, P., and Qiu, J.: Quantifying the effects of the microphysical properties of black carbon on the determination of brown carbon using measurements at multiple wavelengths, *Atmospheric Chemistry and Physics*, 24, 427–448, <https://doi.org/10.5194/acp-24-427-2024>, 2024.
- Mackowski, D.: The extension of the Multiple Sphere T Matrix code to include multiple plane boundaries and 2-D periodic systems, *Journal of Quantitative Spectroscopy and Radiative Transfer*, 290, 108 292, <https://doi.org/https://doi.org/10.1016/j.jqsrt.2022.108292>, 2022.
- Mackowski, D. and Mishchenko, M.: A multiple sphere T-matrix Fortran code for use on parallel computer clusters, *Journal of Quantitative Spectroscopy and Radiative Transfer*, 112, 2182–2192, <https://doi.org/https://doi.org/10.1016/j.jqsrt.2011.02.019>, polarimetric Detection, Characterization, and Remote Sensing, 2011.
- Mikhailov, E. F., Vlasenko, S. S., Podgorny, I. A., Ramanathan, V., and Corrigan, C. E.: Optical properties of soot–water drop agglomerates: An experimental study, *Journal of Geophysical Research: Atmospheres*, 111, <https://doi.org/https://doi.org/10.1029/2005JD006389>, 2006.
- Molod, A., Takacs, L., Suarez, M., and Bacmeister, J.: Development of the GEOS-5 atmospheric general circulation model: evolution from MERRA to MERRA2, *Geoscientific Model Development*, 8, 1339–1356, <https://doi.org/10.5194/gmd-8-1339-2015>, 2015.



- Moteki, N. and Kondo, Y.: Method to measure time-dependent scattering cross sections of particles evaporating in a laser beam, *Journal of Aerosol Science*, 39, 348–364, <https://doi.org/https://doi.org/10.1016/j.jaerosci.2007.12.002>, 2008.
- 440 Myhre, G., Samset, B. H., Schulz, M., Balkanski, Y., Bauer, S., Berntsen, T. K., Bian, H., Bellouin, N., Chin, M., Diehl, T., Easter, R. C., Feichter, J., Ghan, S. J., Hauglustaine, D., Iversen, T., Kinne, S., Kirkevåg, A., Lamarque, J.-F., Lin, G., Liu, X., Lund, M. T., Luo, G., Ma, X., van Noije, T., Penner, J. E., Rasch, P. J., Ruiz, A., Seland, Ø., Skeie, R. B., Stier, P., Takemura, T., Tsigaridis, K., Wang, P., Wang, Z., Xu, L., Yu, H., Yu, F., Yoon, J.-H., Zhang, K., Zhang, H., and Zhou, C.: Radiative forcing of the direct aerosol effect from AeroCom Phase II simulations, *Atmospheric Chemistry and Physics*, 13, 1853–1877, <https://doi.org/10.5194/acp-13-1853-2013>, 2013.
- 445 Naseri, A., Corbin, J., and Olfert, J.: Comparison of the LEO and CPMA-SP2 techniques for black-carbon mixing-state measurements, *EGUsphere*, 2023, 1–30, <https://doi.org/10.5194/egusphere-2023-2216>, 2023.
- Peng, J., Hu, M., Guo, S., Du, Z., Zheng, J., Shang, D., Zamora, M. L., Zeng, L., Shao, M., Wu, Y.-S., Zheng, J., Wang, Y., Glen, C. R., Collins, D. R., Molina, M. J., and Zhang, R.: Markedly enhanced absorption and direct radiative forcing of black carbon under polluted urban environments, *Proceedings of the National Academy of Sciences*, 113, 4266–4271, <https://doi.org/10.1073/pnas.1602310113>, 2016.
- 450 Petzold, A. and Schönlinner, M.: Multi-angle absorption photometry—a new method for the measurement of aerosol light absorption and atmospheric black carbon, *Journal of Aerosol Science*, 35, 421–441, <https://doi.org/https://doi.org/10.1016/j.jaerosci.2003.09.005>, 2004.
- R. S. Gao, J. P. Schwarz, K. K. K. D. W. F. L. A. W. T. L. T. J. R. S. J. G. S. E. S. C. J.-H. H. P. D. T. B. O. and Worsnop, D. R.: A Novel Method for Estimating Light-Scattering Properties of Soot Aerosols Using a Modified Single-Particle Soot Photometer, *Aerosol Science and Technology*, 41, 125–135, <https://doi.org/10.1080/02786820601118398>, 2007.
- 455 Randerson, J., Van Der Werf, G., Giglio, L., Collatz, G., and Kasibhatla, P.: Global Fire Emissions Database, Version 4,(GFEDv4), ORNL DAAC, Oak Ridge, Tennessee, USA, 2018.
- Sand, M., Samset, B. H., Myhre, G., Glib, J., Bauer, S. E., Bian, H., Chin, M., Checa-Garcia, R., Ginoux, P., Kipling, Z., Kirkevåg, A., Kokkola, H., Le Sager, P., Lund, M. T., Matsui, H., van Noije, T., Olivieri, D. J. L., Remy, S., Schulz, M., Stier, P., Stjern, C. W., Takemura, T., Tsigaridis, K., Tsyro, S. G., and Watson-Parris, D.: Aerosol absorption in global models from AeroCom phase III, *Atmospheric Chemistry and Physics*, 21, 15929–15947, <https://doi.org/10.5194/acp-21-15929-2021>, 2021.
- Schnaiter, M., Linke, C., Möhler, O., Naumann, K.-H., Saathoff, H., Wagner, R., Schurath, U., and Wehner, B.: Absorption amplification of black carbon internally mixed with secondary organic aerosol, *Journal of Geophysical Research: Atmospheres*, 110, <https://doi.org/https://doi.org/10.1029/2005JD006046>, 2005.
- Schulz, M., Textor, C., Kinne, S., Balkanski, Y., Bauer, S., Berntsen, T., Berglen, T., Boucher, O., Dentener, F., Guibert, S., Isaksen, I. S. A., Iversen, T., Koch, D., Kirkevåg, A., Liu, X., Montanaro, V., Myhre, G., Penner, J. E., Pitari, G., Reddy, S., Seland, Ø., Stier, P., and Takemura, T.: Radiative forcing by aerosols as derived from the AeroCom present-day and pre-industrial simulations, *Atmospheric Chemistry and Physics*, 6, 5225–5246, <https://doi.org/10.5194/acp-6-5225-2006>, 2006.
- Schwarz, J. P., Gao, R. S., Fahey, D. W., Thomson, D. S., Watts, L. A., Wilson, J. C., Reeves, J. M., Darbeheshti, M., Baumgardner, D. G., Kok, G. L., Chung, S. H., Schulz, M., Hendricks, J., Lauer, A., Kärcher, B., Slowik, J. G., Rosenlof, K. H., Thompson, T. L., Langford, A. O., Loewenstein, M., and Aikin, K. C.: Single-particle measurements of midlatitude black carbon and light-scattering aerosols from the boundary layer to the lower stratosphere, *Journal of Geophysical Research: Atmospheres*, 111, D16207, <https://doi.org/https://doi.org/10.1029/2006JD007076>, 2006.
- 470 Skorupski, K., Mroczka, J., Wriedt, T., and Riefler, N.: A fast and accurate implementation of tunable algorithms used for generation of fractal-like aggregate models, *Physica A: Statistical Mechanics and its Applications*, 404, 106–117, <https://doi.org/https://doi.org/10.1016/j.physa.2014.02.072>, 2014.
- 475



- Sorensen, C. M.: Light Scattering by Fractal Aggregates: A Review, *Aerosol Science and Technology*, 35, 648–687, <https://doi.org/10.1080/02786820117868>, 2001.
- Sumlin, B. J., Heinson, W. R., and Chakrabarty, R. K.: Retrieving the aerosol complex refractive index using PyMieScatt: A Mie computational package with visualization capabilities, *Journal of Quantitative Spectroscopy and Radiative Transfer*, 205, 127–134, <https://doi.org/https://doi.org/10.1016/j.jqsrt.2017.10.012>, 2018.
- 480 Textor, C., Schulz, M., Guibert, S., Kinne, S., Balkanski, Y., Bauer, S., Bernsten, T., Berglen, T., Boucher, O., Chin, M., Dentener, F., Diehl, T., Easter, R., Feichter, H., Fillmore, D., Ghan, S., Ginoux, P., Gong, S., Grini, A., Hendricks, J., Horowitz, L., Huang, P., Isaksen, I., Iversen, I., Kloster, S., Koch, D., Kirkevåg, A., Kristjansson, J. E., Krol, M., Lauer, A., Lamarque, J. F., Liu, X., Montanaro, V., Myhre, G., Penner, J., Pitari, G., Reddy, S., Seland, Ø., Stier, P., Takemura, T., and Tie, X.: Analysis and quantification of the diversities of aerosol life cycles within AeroCom, *Atmospheric Chemistry and Physics*, 6, 1777–1813, <https://doi.org/10.5194/acp-6-1777-2006>, 2006.
- 485 Thouy, R. and Jullien, R.: A cluster-cluster aggregation model with tunable fractal dimension, *Journal of Physics A: Mathematical and General*, 27, 2953, <https://doi.org/10.1088/0305-4470/27/9/012>, 1994.
- Wang, J., Wang, J., Cai, R., Liu, C., Jiang, J., Nie, W., Wang, J., Moteki, N., Zaveri, R. A., Huang, X., Ma, N., Chen, G., Wang, Z., Jin, Y., Cai, J., Zhang, Y., Chi, X., Holanda, B. A., Xing, J., Liu, T., Qi, X., Wang, Q., Pöhlker, C., Su, H., Cheng, Y., Wang, S., Hao, J., Andreae, M. O., and Ding, A.: Unified theoretical framework for black carbon mixing state allows greater accuracy of climate effect estimation, *Nature Communications*, 14, 2703, <https://doi.org/10.1038/s41467-023-38330-x>, 2023.
- 490 Wang, Y., Liu, F., He, C., Bi, L., Cheng, T., Wang, Z., Zhang, H., Zhang, X., Shi, Z., and Li, W.: Fractal Dimensions and Mixing Structures of Soot Particles during Atmospheric Processing, *Environmental Science & Technology Letters*, 4, 487–493, <https://doi.org/10.1021/acs.estlett.7b00418>, 2017.
- 495 Wang, Y., Li, W., Huang, J., Liu, L., Pang, Y., He, C., Liu, F., Liu, D., Bi, L., Zhang, X., and Shi, Z.: Nonlinear Enhancement of Radiative Absorption by Black Carbon in Response to Particle Mixing Structure, *Geophysical Research Letters*, 48, e2021GL096437, <https://doi.org/https://doi.org/10.1029/2021GL096437>, e2021GL096437 2021GL096437, 2021a.
- Wang, Y., Li, W., Huang, J., Liu, L., Pang, Y., He, C., Liu, F., Liu, D., Bi, L., Zhang, X., and Shi, Z.: Nonlinear Enhancement of Radiative Absorption by Black Carbon in Response to Particle Mixing Structure, *Geophysical Research Letters*, 48, e2021GL096437, <https://doi.org/https://doi.org/10.1029/2021GL096437>, e2021GL096437 2021GL096437, 2021b.
- 500 Wang, Y., Pang, Y., Huang, J., Bi, L., Che, H., Zhang, X., and Li, W.: Constructing Shapes and Mixing Structures of Black Carbon Particles With Applications to Optical Calculations, *Journal of Geophysical Research: Atmospheres*, 126, e2021JD034620, <https://doi.org/https://doi.org/10.1029/2021JD034620>, e2021JD034620 2021JD034620, 2021c.
- Wentzel, M., Gorzawski, H., Naumann, K.-H., Saathoff, H., and Weinbruch, S.: Transmission electron microscopical and aerosol dynamical characterization of soot aerosols, *Journal of Aerosol Science*, 34, 1347–1370, [https://doi.org/https://doi.org/10.1016/S0021-8502\(03\)00360-4](https://doi.org/https://doi.org/10.1016/S0021-8502(03)00360-4), intercomparison of Soot Measurement Techniques, 2003a.
- 505 Wentzel, M., Gorzawski, H., Naumann, K.-H., Saathoff, H., and Weinbruch, S.: Transmission electron microscopical and aerosol dynamical characterization of soot aerosols, *Journal of aerosol science*, 34, 1347–1370, 2003b.
- Woźniak, M.: CHARACTERIZATION OF NANOPARTICLE AGGREGATES WITH LIGHT SCATTERING TECHNIQUES, Theses, Aix-Marseille Université, <https://tel.archives-ouvertes.fr/tel-00747711>, 2012.
- 510 Wu, Y., Cheng, T., Zheng, L., Zhang, Y., and Zhang, L.: Particle size amplification of black carbon by scattering measurement due to morphology diversity, *Environmental Research Letters*, 18, 024011, <https://doi.org/10.1088/1748-9326/acaede>, 2023.

<https://doi.org/10.5194/egusphere-2024-1155>

Preprint. Discussion started: 14 May 2024

© Author(s) 2024. CC BY 4.0 License.



- Zhang, R., Khalizov, A. F., Pagels, J., Zhang, D., Xue, H., and McMurry, P. H.: Variability in morphology, hygroscopicity, and optical properties of soot aerosols during atmospheric processing, *Proceedings of the National Academy of Sciences*, 105, 10 291–10 296, 2008.
- 515 Zhang, X., Mao, M., Yin, Y., and Wang, B.: Numerical Investigation on Absorption Enhancement of Black Carbon Aerosols Partially Coated With Nonabsorbing Organics, *Journal of Geophysical Research: Atmospheres*, 123, 1297–1308, <https://doi.org/https://doi.org/10.1002/2017JD027833>, 2018.

<https://doi.org/10.5194/egusphere-2024-1155>

Preprint. Discussion started: 14 May 2024

© Author(s) 2024. CC BY 4.0 License.



Data availability. The data can be requested from the corresponding author.

Author contributions. JL and MH conceived the presented idea. JL developed the models, performed the computations, and wrote the paper. 520 JQ, KL, HH, YS and XG verified the simulation methods and results. MH and JQ revised the paper and supervised the findings of this work. All authors discussed the results and contributed to the final paper.

Competing interests. The authors declare that they have no conflict of interest.